Original Article

SOCKET SHIELD TECHNIQUE: STRESS DISTRIBUTION ANALYSIS

Wei He[1], *Shanyan Zhou*[2], *Yinan Wang*[2], *Nivetha Kumar*[1]*, *Fangyan Lu*[2]

[1]*Department of Stomatology, The People's Hospital of Pingyang(Pingyang Hospital of Wenzhou Medical University), Wenzhou, 325400 Zhejiang, PR China. Kumar.nivetha.in@yahoo.com*

[2]*Department of Stomatology, The First Affiliated Hospital of Wenzhou Medical University, Wenzhou, 325015 Zhejiang, PR China.*

Received: 21 December 2024; **Revised:** 16 March 2025; **Accepted:** 18 March 2025 https://doi.org/10.51847/IqF65CiRmM

ABSTRACT

To analyze through finite element analysis the stress distribution in peri-implant bone tissues, implants, and prosthetic components induced by the socket shield (SS) technique in comparison to other techniques used to treat tooth loss. A three-dimensional model of a superior central incisor crown supported by implant was modeled and three different placement conditions were simulated: SS – 2.0-mm-thick root dentin fragment positioned between the alveolar buccal wall and implant; heterologous bone graft (HBG) – bovine bone graft positioned the alveolar buccal wall and implant; and control (C) – implant fully placed in bone tissue of a healed alveolus. The model was restricted at the lateral surfaces of the bone tissue and the following loads were simulated: Both oblique (45°) loads of 100 N on the lingual surface of the crown (maximal habitual intercuspation) and 25.5 N on the incisal edge of the crown (tooth contact during mandibular protrusion) were simultaneously applied. Tensile stress, shear stress, compression, and displacement were analyzed in the cortical bone, trabecular bone, dentin root fragment, and bone graft; while equivalent von Mises stresses were quantified in the implant and prosthetic components. Stress values of SS and HBG in the bone tissues were higher than C, while slight differences within models were observed for dentin root fragment, bone graft, implant, and prosthetic components. The SS technique presented the highest stress concentration in the peri-implant tissues.

Key words: Alveolar ridge, Finite element analysis, Implant placement, Stress.

Introduction

Experimental studies in humans have shown the physiological alveolar bone resorption after single or multiple tooth extractions and the consequent reduction in horizontal and vertical dimensions of alveolar ridges [1-4], which may impair implant placement in terms of moderate esthetic results or the necessity of further tissue reconstructions [5-7]. Ridge alterations following tooth extractions seem related to periodontal ligament loss and trauma in the buccal bone plate that presents more pronounced resorption than the lingual/palatal portion of the alveolus [8].

In particular for anterior teeth, different techniques have been proposed to stabilize alveolar hard and soft tissues and to obtain satisfactory esthetic results [9]. Several regenerative biomaterials, such as tissue grafts (autogenous, heterologous, or allograft) and growth-promoting factors, have been tested with the aim of preserving the alveolar ridge volume after tooth extractions [10-14].

In 2010, Hürzeler *et al*. [15] proposed a novel approach to maintain the buccal bone plate and to improve esthetic predictability. The so-called socket shield (SS) technique consists in removing the dental crown, mesiodistal sectioning of the root, extraction of the lingual root fragment, maintenance of the residual buccal root portion in contact with the buccal bone plate and immediate implant placement. The beneficial effect of the root fragment maintenance has been histologically demonstrated by the apposition of cementum on the implant surfaces. Following the same concept of partial root extraction, Gluckman *et al*. [16, 17] also suggested filling the space between the buccal root fragment and the implant with a particulate bone graft. Mitsias *et al*. [18] and Siormpas *et al*. [19] renamed the technique to *Root Membrane* and claimed that the bone graft would not be necessary since the preservation of the buccal bone plate is based on the maintenance of the periodontal ligament and part of the root.

Another positive factor associated with the SS technique is the maintenance of the interdental papillae, which is influenced by the condition of the peri-implant tissues. Cherel and Etienne [7], Kan and Rungcharassaeng [20] and Tan *et al*. [21] have shown that a small root fragment kept in the coronal portion of the alveolus can protect the buccal, mesial, and distal bone plates after immediate implant placement; however, a recent animal study demonstrated bone loss between 3.1 and 6 mm after 4 months [5]. Therefore, more scientific pieces of evidence regarding the safe use of the SS technique are still lacking [22].

Buccal bone losses due to vertical fractures or periodontitis and root caries are contraindications for the SS technique [22, 23]. Late migration and internal or external exposure of the root fragment figure as among the adverse reactions that cause inflammation of epithelial tissue [24, 25]. A current systematic review on the SS technique reported histologic evidence of rapid bone loss, failure of osseointegration, the formation of cementum, periodontal ligament, or fibrous tissue on implant surfaces in proximity to the root fragmented [26].

To prevent loss and achieve the long-term clinical success of dental implants, it is essential to understand the biomechanical behavior between bone tissue and implant and the influence of stress distribution around implants [27–30]. Three-dimensional (3D) finite element analysis (FEA) is an efficient technique to evaluate the extent of micromotions and peri-implant bone strain distribution [31]. As an appropriate numerical method for analyzing complex biological structures, FEA has been widely used to evaluate the effect of several parameters in the peri-implant region (e.g., implant geometry, prosthesis design, stress, and strain distribution) [32].

The quality of adjacent bone tissue influences both stress distribution and biomechanical behavior of implants; hence, the success or failure of dental implants is dependent on how stresses are transferred to the surrounding bone tissues [27, 33]. The stress distribution induced by the SS technique should be investigated by considering critical parameters such as bone anatomy and density, implant positioning, and different loads. To date, there are no studies in the literature regarding stress patterns on both implant-prosthesis complex and peri-implant bone to support the use and to predict the long-term performance of SS technique [22, 34, 35]. Therefore, this study analyzed through FEA the stress distribution in peri-implant bone tissues, implants, and prosthetic components induced by the SS technique in comparison to other techniques used to treat tooth loss [36–38].

Materials and Methods

Computed tomographic images (KODAK 9000 3D Extra Oral Imaging System, Carestream Dental LLC, Atlanta, GA, USA) acquired from the anterior region of partially edentulous maxilla were reconstructed and exported to stereolithographic files (.stl) with the aid of specific software (InVesalius 3.0, Center for Information Technology Renato Archer, Campinas, São Paulo, Brazil). After soft tissue segmentation, files of cortical and trabecular bone tissues were imported into a computer-aided design software (SolidWorks Premium 2011, 3Dtech-Solidworks, Concord, MA, USA); next, 3D models with 15-mm-high trabecular bone surrounded by a uniform 2-mm-thick layer of cortical bone (corresponding to type III bone tissue typically found in the anterior maxilla) were generated [39]. In addition, a Ø4.0 mm × 13.0 mm cylindrical body implant with conical apex and Morse taper connection (CM Titamax EX, Neodent, Curitiba, PR, Brazil), a Ø3.3 x 6.0 mm prosthetic abutment with 2.5 mm collar height (CM Universal Abutment, Neodent, Curitiba, PR, Brazil), a feldspathic porcelain veneered-zirconia crown (0.5-mm-thick zirconia and 1.5-mm-thick feldspathic porcelain) and a 50-μm-thick resin cement layer (Panavia F, Kuraray, Okayama, Japan) were also modeled. Different implant placement conditions were simulated **(Figure 1)**: SS: 2-mm-thick root dentin fragment with 0.25-mm-thick periodontal ligament positioned between the alveolar buccal wall and implant; heterologous bone graft (HBG): filling of the gap between alveolar buccal wall and implant with a bovine bone graft (Bio-Oss, Geistlich, Wolhusen, Switzerland); Control (C): implant fully placed in bone tissue of a healed alveolus.

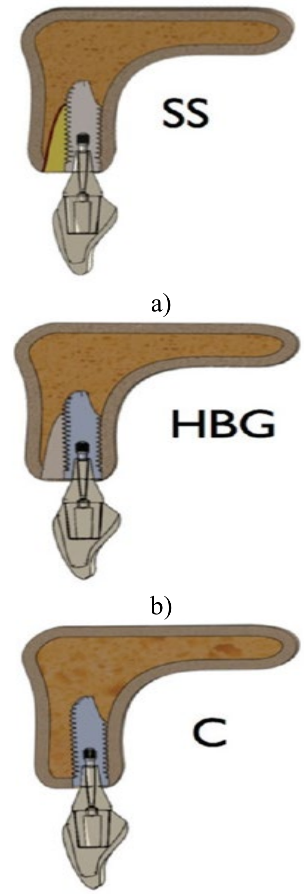

c)

Figure 1. Scheme of the different implant placement conditions and experimental models. SS: Socket shield; HBG: Heterologous bone graft; C: Control

The files (.iges) were exported to FEA software developed for stress analysis (Ansys Workbench 13.0, Swanson Analysis Inc., Houston, PA, USA), in which meshes were refined and submitted to a convergence analysis of 5% to confirm the accuracy and to ensure the comparability of results [40, 41]. The mesh consisted of 0.6 mm tetrahedral solid elements and respective nodes **(Table 1)**, while the contact surfaces between the structures were set as bonded. The model was restricted at the lateral surfaces of the bone tissue (x-, y-and z-axis) and the following loads were simulated: a constant force of 100 N obliquely (45°) applied on the lingual surface of the crown (1.5 mm² area) to simulate maximal habitual intercuspation and 25.5 N applied on the incisal edge of the crown (perpendicular to the implant long axis) with the aim to simulate the tooth contact during mandibular protrusion [42]. The software performed a joint analysis of the two loads simultaneously applied **(Figure 2)**.

Table 1. The number of structures, nodes, and elements in each model

Models	Structures	Nodes	Elements
SS	12	242,172	136,386
HBG	10	227,795	129,427
Control	9	210,159	119,853

SS – Socket shield; HBG – Heterologous bone graft

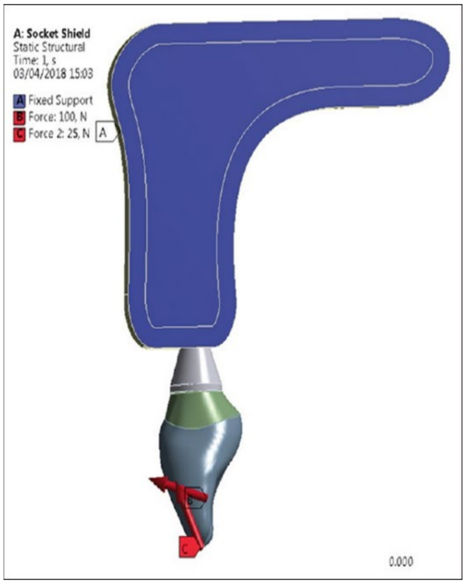

Figure 2. Side view of A: bone tissue as fixed support, B: oblique 100 N and C: 25.5 N loads perpendicularly applied to the implant long axis. N: Newton

Both cortical and trabecular bone tissues were assumed as homogeneous and anisotropic with linear elasticity; while implant, bone graft, root dentine, prosthetic abutment, zirconia, feldspathic porcelain, and resin cement were considered homogeneous and isotropic with linear elasticity. The x-, y-and z-axis of the materials correspond to the coordinates of the system. The Young's Modulus and Poisson's ratio of each material are described in **Tables 2 and 3**.

Table 2. Mechanical properties of cortical and trabecular bone tissues in accordance with Huang *et al*. [40] and Lan *et al*. [43]

Young's modulus (MPa)	Shear modulus (MPa)	Poisson's ratio
Cortical		
E_x 12.600	G_{xy} 4.850	V_{xy} 0.30
E_y 12.600	G_{yz} 5.700	V_{yz} 0.39
E_z 19.400	G_{xz} 5.700	V_{xz} 0.39
Trabecular		
E_x 1.150	G_{xy} 6.800	V_{xy} 0.001
E_y 2.100	G_{yz} 4.340	V_{yz} 0.32
E_z 1.150	G_{xz} 6.800	V_{xz} 0.05

MPa – Megapascal

Table 3. Young's modulus and Poisson's ratio of all materials modeled

Materials	Young's modulus (GPa)	Poisson's ratio	Reference
Feldspathic porcelain	70	0.19	Coelho *et al.* [44]
Zirconia	205	0.22	Coelho *et al.* [44]
Resin cement	18.3	0.33	Li *et al.* [45]
Titanium (implants and components)	110	0.33	Cruz *et al.* [46]
Dentin	20	0.31	Dejak and Mlotkowski [47]
Periodontal ligament	0.05	0.45	Rees and Jacobsen [48]
Bovine bone graft	11	0.30	Fanuscu *et al.* [49]

GPa – Gigapascal

The results were both quantitatively (tensile stress, shear, compression, and displacement were assessed in the peri-implant bone tissues, dentin, and bone graft; while the equivalent von Mises stresses were quantified in the implant and prosthetic components) and qualitatively analyzed (visual comparison of images with color gradients and standardized scales).

Results and Discussion

Quantitative results observed in the different structures are described in **Table 4**. The tensile stress values of SS and HBG in the cortical bone were higher (approximately 170%) than C. Similarly, SS and HBG presented shear stress values around 80% higher than the C; however, compression and displacement values in the cortical bone were similar among the models.

Table 4. Values of tension, shear, compression, displacement and von Mises stresses in different structures and models

	SS	HBG	Control
Tension (MPa)			
Cortical bone	156	137	52
Trabecular bone	21.6	16	5

Dentin/graft	32	28	-
Shear (MPa)			
Cortical bone	42	37	21
Trabecular bone	6.5	4.4	1.6
Dentin/graft	11.6	11.2	-
Compression (MPa)			
Cortical bone	68	69	57
Trabecular bone	17	17	9.2
Dentin/graft	50	30	-
Displacement (µm)			
Cortical bone	18	16	13
Trabecular bone	15	13	12
Dentin/graft	24	21	-
von Mises (MPa)			
Implant	413	428	409
Screw	380	389	358
Abutment	1006	985	997

SS – Socket shield; HBG – Heterologous bone graft; Mpa – Megapascal; µm – Micrometer

Considering the trabecular bone, tensile, shear, and compression stress values observed in SS and HBG were higher (approximately 200%) than C, while displacement remained similar among the models.

The root dentin simulated in SS induced tensile stress values (32 MPa) slightly higher than the biomaterial simulated in the HBG (28 MPa), while shear stress values were very similar (12.5 and 11.2 MPa, respectively). Compression stress values in dentin were higher in comparison to the simulated bone graft (50 and 30 MPa, respectively). Regardless of the experimental model, the values of equivalent *von Mises* stress in implant, screw, and prosthetic abutment showed slight variation (<10%).

The qualitative evaluations of the models are shown in **Figures 3-6**. In SS and HBG, the maximum principal stress points were observed at the interface between lingual cortical bone and implant coronal area, while the maximum stress in the C was found at the interface between the buccal alveolar ridge and implant platform/coronal threads. Regarding the screws in all models, the stresses were concentrated on the buccal face and at the level of the implant platform. Similarly, the prosthetic abutments of all models presented maximum principal stresses in the region in contact with the implant platform; therefore, the internal aspect of the Morse taper connection showed the maximum stresses concentrated in the implants.

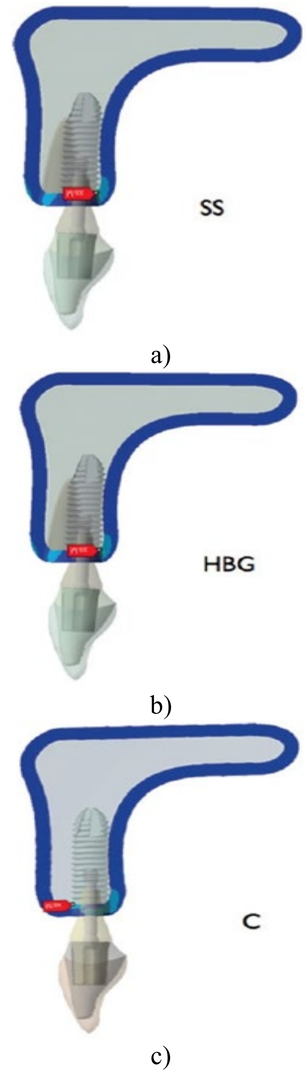

Figure 3. Cross-sectional view of the stress distribution in cortical bone for each model (red arrows indicate maximum principal stress points). Max: Maximum, SS: Socket shield; HBG: Heterologous bone graft; C: Control

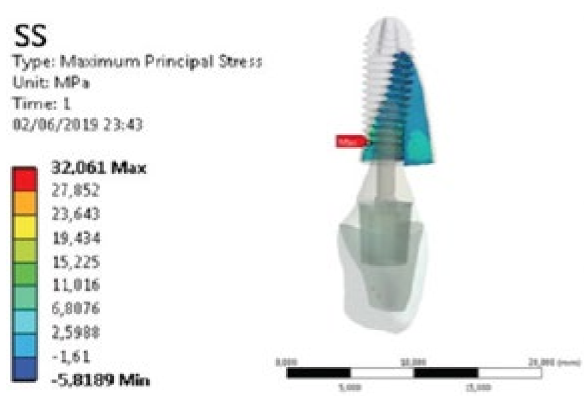

a)

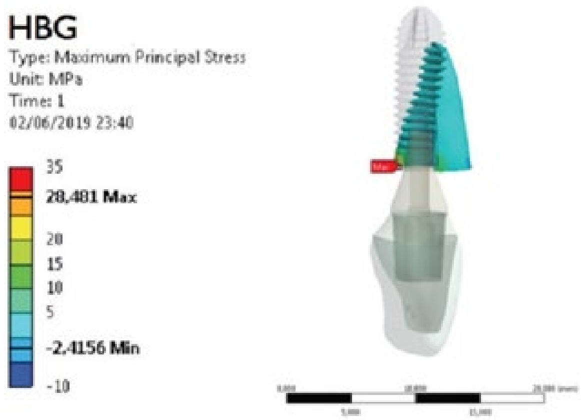

b)

Figure 4. Tensile stress distribution in SS and HBG models (red arrows indicate maximum principal stress points). MPa: Megapascal; Min: Minimum; Max: Maximum, SS: Socket shield, HBG: Heterologous bone graft

a)

b)

Figure 5. Shear stress distribution in SS and HBG models (red arrows indicate maximum principal stress points). MPa: Megapascal; Min: Minimum; Max: Maximum, SS: Socket shield, HBG: Heterologous bone graft

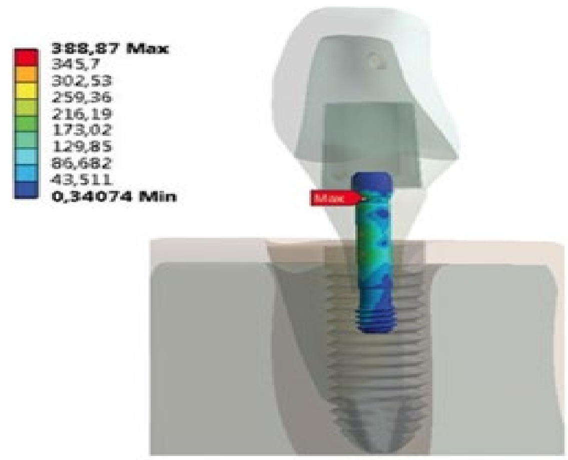

a)

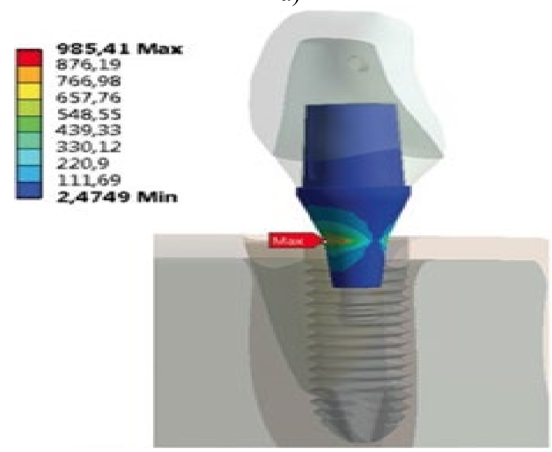

b)

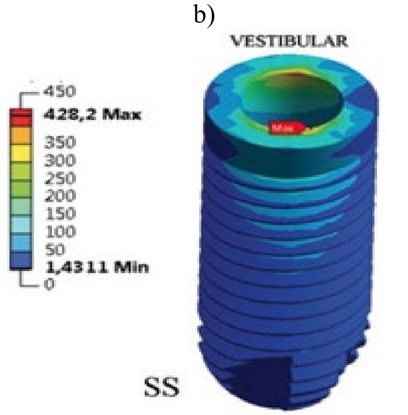

c)

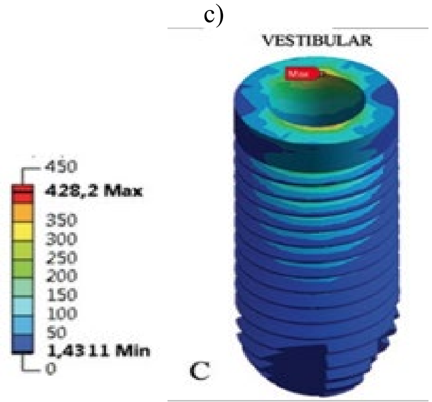

d)

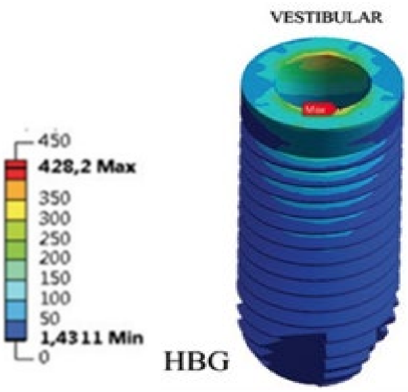

e)

Figure 6. Equivalent *von Mises* stress distribution in screws, prosthetic abutments and implants was similar among the models (red arrows indicate the points of maximum stress). Min: Minimum; Max: Maximum, SS: Socket shield; HBG: Heterologous bone graft; C: Control

A key factor for the success of dental implants is the masticatory tension to which bone tissue is submitted [50]. According to Newton's third law, chewing forces transmitted to prosthetic restoration are transformed into energy that is distributed in certain amounts through the implant-prosthesis complex and peri-implant bone tissue [51]. The stress transfer to the interface between bone tissue and implants placed in the region of central incisors is especially relevant due to the greater biomechanical risk of failure. So far, only short-term clinical trials reported the success of the SS technique; therefore, we performed an FEA on the biomechanical behavior of the bone tissue adjacent to an implant placed in the region of central incisors [52, 53]. In both SS and HBG, tensile, shear, and compression stress values in the cortical and trabecular bones in both SS and HBG were higher than the C. In contrast, displacement values and equivalent *von Mises* stress in the implant-prosthesis complex were only slightly different among models.

The tensile stress values in the cortical bone were higher in the SS and HBG in comparison to C, which may be explained by the smaller contact area between bone tissue and implant in addition to differences in the mechanical properties of bone tissue, bone graft and, dentin; the latter with the lower modulus of elasticity [54]. The approximate mechanical properties of the bone graft and dentin may explain the similar results. In comparison to trabecular bone, the cortical bone presents a higher modulus of elasticity, is more resistant to deformation and can bear more load [55]. The maximum tensile stress values in trabecular bone followed the same trend among models; the low elastic modulus of trabecular bone acts as a stress breaker that better dissipates the chewing forces [56]. Tension, shear, compression and, displacement criteria were analyzed to evaluate the biomechanical behavior of fragile structures such as dentin, bone graft, cortical and, trabecular bone [57]. The *von Mises* criterion was used for implant, screw, and prosthetic abutment since it is an adequate stress criterion to evaluate the tensional behavior of ductile materials such as titanium. The equivalent *von Mises* stress represents the set of principal stresses that act on a solid element; thus, both compressive and tensile stresses are expressed in a single value and the stress distribution is easily visualized [58]. Differently from C, in which the maximum tensile and shear stresses were observed at the interface between the implant and buccal bone tissue (implant platform/coronal threads), both SS and HBG were characterized by maximum stresses concentrated at the interface between lingual cortical bone and implant coronal area; this result is expected since the oblique load tends to compress the buccal aspect of the implant-supported crown and to induce tension on the palatal aspect of the implant.

Despite the satisfactory results of the SS technique, a recent systematic review based on histological studies in animals reported complications in 58 (82.86%) out of 70 implants; 54.55% of the cases presented partial buccal bone plate loss and 27.27% were associated with failure in implant osseointegration. Thirty-three (24.26%) among 136 implants reported in 21 clinical cases presented complications; 78.78% of the cases were found with partial buccal bone plate loss and 12.12% presented root fragment exposure. Even though many case reports have provided positive short-term outcomes (between three and 40 months), long-term and high-quality studies are needed to predict the longevity success of the technique [26]. In our study, displacement of the cylindrical implant with Morse taper connection was similar among models **(Table 4)**; however, distinct results could be observed in the case of cortical bone anchorage, which is effective in limiting implant displacement [56]. Following Sugiura *et al*. [54], implant configuration has a limited influence on micromotion; in addition, optimal osseointegration simulated in this study differs from the clinical reality in which implants are placed in fresh alveoli [59–62].

Considering that elevated stress levels may cause failure in the osseointegration of implants [63], it seems critical that cortical and trabecular bone tensile stress values observed in SS and HBG were 170% and 200% higher than values found in C Further controlled clinical trials with long-term follow-ups are necessary to confirm these findings and determine the safety of the SS technique. It should be considered that the properties of the bone graft material simulated in the HBG are likely to change over time due to contact with bone tissue, whereas the dentin fragment simulated in the SS should preserve its characteristics as shown by histological evidence [22, 64]. Therefore, in the long run, the characteristics of the HBG should become similar to those of while the high tensile stress in peri-implant tissue observed for SS tends to remain unchanged.

The FEA has been often used to understand oral biomechanics and to verify hypotheses on the relationship between mechanical loading to peri-implant bone responses

[65]. The validity of FEA depends on model geometry, as well as on material properties and conditions at the boundary and the interface between bone and implant, especially for the simulation of immediately loaded implants [54]. This method can predict the stress behavior of different structures [66]; however, the fact that some of the investigated structures were assumed as homogeneous and isotropic with linear elasticity may be considered a study limitation [43, 44]. While bone tissue has heterologous and anisotropic characteristics, the periodontal ligament is a viscoelastic material. In addition, the analysis of the models was linear, and thus different results are expected in the case of non-linear analysis. In this study, the buccal threads of the implant were in contact with the dentin of the shield. It could be argued that the implant could be far from the shield and bone would be in between the implant and the dentin shield [67]. In order to avoid unreal stress accumulation in a thin bone layer in this FEA analysis, the authors preferred to simulate the condition of contact between the implant and dentin shield. Considering the limitations related to these constraints of a computer simulation, it is possible to conclude that the implant placement technique influences the peri-implant bone stress distribution and the SS technique presented the highest stress values.

Conclusion

According to the 26 studies included in the systematic review, 72% of the candidates were with malocclusion in Saudi Arabia. The prevalence of Class 1, 2, and 3 malocclusions were 66.51%, 17.70%, and 15.79%, respectively. In both male and female participants, the prevalence of Class1 malocclusion was the highest followed by class 2 and 3 malocclusions.

Acknowledgments: None

Conflict of interest: None

Financial support: None

Ethics statement: None

References

1. Chen CL, Pan YH. Socket shield technique for ridge preservation: a case report. J Prosthodont Implant 2013;2(2):16–21.
2. Chen J, Zhang Z, Chen X, Zhang X. Influence of custom-made implant designs on the biomechanical performance for the case of immediate post-extraction placement in the maxillary esthetic zone: a finite element analysis. Comput Methods Biomech Biomed Engin. 2017;20(6):636–44.
3. Hämmerle CH, Araújo MG, Simion M. Osteology consensus group 2011. Evidence-based knowledge on the biology and treatment of extraction sockets. Clin Oral Implants Res. 2012;23(Suppl 5):80–2.
4. Parelli J, Abramowicz S. Immediate placement and immediate loading: surgical technique and clinical pearls. Dent Clin North Am. 2015;59(2):345–55.
5. Calvo-Guirado JL, Troiano M, López-López PJ, Ramírez-Fernandez MP, de Val JE, Marin JM, et al. Different configuration of socket shield technique in peri-implant bone preservation: an experimental study in dog mandible. Ann Anat. 2016;208:109–15.
6. Calvo-Guirado JL, Benítez-García JA, MatéSánchez de Val JE, Pérez-Albacete Martínez C, Gehrke SA, Delgado-Ruiz R, et al. Socket-shield technique: the influence of the length of the remaining buccal segment of healthy tooth structure on peri-implant bone and socket preservation. A study in dogs. Ann Anat. 2019;221:84–92.
7. Cherel F, Etienne D. Papilla preservation between two implants: a modified socket-shield technique to maintain the scalloped anatomy? A case report. Quintessence Int. 2014;45(1):23–30.
8. Araújo MG, Sukekava F, Wennström JL, Lindhe J. Ridge alterations following implant placement in fresh extraction sockets: an experimental study in the dog. J Clin Periodontol. 2005;32(6):645–52.
9. Avila-Ortiz G, Elangovan S, Kramer KW, Blanchette D, Dawson DV. Effect of alveolar ridge preservation after tooth extraction: a systematic review and meta-analysis. J Dent Res. 2014;93(10):950–8.
10. Abadzhiev M, Nenkov P, Velcheva P. Conventional immediate implant placement and immediate placement with socket-shield technique –Which is better. Int J Clin Med. 2014;1(5):176–80.
11. Barone A, Toti P, Quaranta A, Alfonsi F, Cucchi A, Calvo-Guirado JL, et al. Volumetric analysis of remodelling pattern after ridge preservation comparing use of two types of xenografts. A multicentre randomized clinical trial. Clin Oral Implants Res. 2016;27(11):e105–15.
12. Glocker M, Attin T, Schmidlin PR. Ridge preservation with modified “socket-shield”technique: a methodological case series. Dent J. 2014;2(1):11–21.
13. Lindhe J, Cecchinato D, Donati M, Tomasi C, Liljenberg B. Ridge preservation with the use of deproteinized bovine bone mineral. Clin Oral Implants Res. 2014;25(7):786–90.
14. Negri B, Zuhr O, Fickl S, Ciurana XR, Navarro Martínez JM, Blanco VM. Socket seal surgery: clinical uses in implant dentistry and guided bone regeneration procedures for single tooth replacement in the esthetic zone. Quintessence Int. 2016;47(2):123–39.
15. Hürzeler MB, Zuhr O, Schupbach P, Rebele SF, Emmanouilidis N, Fickl S. The socket-shield technique: a proof-of-principle report. J Clin Periodontol. 2010;37(9):855–62.
16. Gluckman H, Salama M, Du Toit J. Partial extraction therapies (PET) Part 1: maintaining alveolar ridge contour at pontic and immediate implant sites. Int J Periodontics Restorative Dent. 2016;36(5):681–7.

17. Gluckman H, Salama M, Du Toit J. Partial extraction therapies (PET) Part 2: procedures and technical aspects. Int J Periodontics Restorative Dent. 2017;37(3):377–85.
18. Mitsias ME, Siormpas KD, Kotsakis GA, Ganz SD, Mangano C, Iezzi G. The root membrane technique: human histologic evidence after five years of function. Biomed Res Int. 2017;2017(1):1–8.
19. Siormpas KD, Mitsias ME, Kontsiotou-Siormpa E, Garber D, Kotsakis GA. Immediate implant placement in the esthetic zone utilizing the “root-membrane”technique: clinical results up to 5 years postloading. Int J Oral Maxillofac Implants. 2014;29(6):1397–405.
20. Kan JY, Rungcharassaeng K. Proximal socket shield for interimplant papilla preservation in the esthetic zone. Int J Periodontics Restorative Dent. 2013;33(1):e24–31.
21. Tan Z, Kang J, Liu W, Wang H. The effect of the heights and thicknesses of the remaining root segments on buccal bone resorption in the socket-shield technique: an experimental study in dogs. Clin Implant Dent Relat Res. 2018;20(3):352–9.
22. Gluckman H, Du Toit J, Salama M. The socket-shield technique to support the buccofacial tissues at immediate implant placement. Int Dent Africa Ed. 2015;5(3):6–14.
23. Mujawar S, Devkar N, Vibhute A, Deshpande M, Mali P. Socket shield technique: a review. Int J Recent Sci Res. 2018;9:27612–5.
24. Gluckman H, Nagy K, Du Toit J. Prosthetic management of implants placed with the socket-shield technique. J Prosthet Dent. 2019;121(4):581–5.
25. Mohammad AA, Elnaem M, Ong SC. Understanding diabetes management among patients in hail city using the health belief model. J Adv Pharm Educ Res. 2024;14(4):28-33. doi:10.51847/AqAVGRxPXc
26. Gharpure AS, Bhatavadekar NB. Current evidence on the socket-shield technique: a systematic review. J Oral Implantol. 2017;43(5):395–403.
27. Dundar S, Topkaya T, Solmaz MY, Yaman F, Atalay Y, Saybak A, et al. Finite element analysis of the stress distributions in peri-implant bone in modified and standard-threaded dental implants. Biotech Biotech Equip. 2016;30(1):127–33.
28. Dorontsev AV, Vorobyeva NV, Kumantsova ES, Shulgin AM, Sharagin VI, Eremin MV. Functional changes in the body of young men who started regular physical activity. J Biochem Technol. 2022;13(1):65-71. doi:10.51847/X03w75Xldo
29. Voiţă-Mekereş F, Manole F, Voiţă IB, Marian P. The Role of Food Biochemistry in the control and prevention of nervous system diseases. J Biochem Technol. 2023;14(2):112-6. doi:10.51847/AtDeJS15Py
30. Ajiboye BO, Famusiwa CD, Oyedare DI, Julius BP, Adewole ZO, Ojo OA, et al. Hibiscus sabdariffa Leaf Extract Enhances Molecular Gene Expression of Insulin and GLP-1 receptors in streptozotocin-induced rats. Spec J Pharmacogn Phytochem Biotechnol. 2024;4:59-73. doi:10.51847/9lS5Ohuhiv
31. Sugiura T, Yamamoto K, Horita S, Murakami K, Tsutsumi S, Kirita T. The effects of bone density and crestal cortical bone thickness on micromotion and peri-implant bone strain distribution in an immediately loaded implant: a nonlinear finite element analysis. J Periodontal Implant Sci. 2016;46(3):152–65.
32. Liao SH, Zhu XH, Xie J, Sohodeb VK, Ding X. Influence of trabecular bone on peri-implant stress and strain based on Micro-CT finite element modeling of beagle dog. Biomed Res Int. 2016;2016:1–11.
33. Kurniawan D, Nor FM, Lee HY, Lim JY. Finite element analysis of bone-implant biomechanics: refinement through featuring various osseointegration conditions. Int J Oral Maxillofac Surg. 2012;41(9):1090–6.
34. Bäumer D, Zuhr O, Rebele S, Schneider D, Schupbach P, Hürzeler M. The socket-shield technique: first histological, clinical, and volumetrical observations after separation of the buccal tooth segment –A pilot study. Clin Implant Dent Relat Res. 2015;17(1):71–82.
35. Bäumer D, Zuhr O, Rebele S, Hürzeler M. Socket Shield Technique for immediate implant placement – Clinical, radiographic and volumetric data after 5 years. Clin Oral Implants Res. 2017;28(11):1450–8.
36. Wal A, Wal P, Pandey A, Vig H, Ved A, Samal HB. Exploring myasthenia gravis subtypes: impact on pregnancy and recent treatment advancements. Interdiscip Res Med Sci Spec. 2023;3(1):26-38. doi:10.51847/LfGflzk9de
37. Muresan GC, Hedesiu M, Lucaciu O, Boca S, Petrescu N. Evaluation of bone turnover indicators before dental implant insertion in osteoporotic patients: a case-control investigation. J Curr Res Oral Surg. 2023;3(1-2023):27-32. doi:10.51847/P4EfMAbJVb
38. Jannath A, Sivapragasam S, Viswanathan K, Sundaram R. Intentional replantation combined with periapical surgery: a case report with one-year follow-up. J Curr Res Oral Surg. 2024;4(1-2024):56-61. doi:10.51847/WzyOlpBh6c
39. Almeida EO, Freitas Júnior AC, Rocha EP, Pessoa RS, Gupta N, Tovar N, et al. Critical aspects for mechanical simulation in dental implantology Moratal D. Finite Element Analysis: From Biomedical Applications to Industrial Developments London InTechopen; 2012. p. 81–106.
40. Huang HL, Chang CH, Hsu JT, Fallgatter AM, Ko CC. Comparison of implant body designs and threaded designs of dental implants: a 3-dimensional finite element analysis. Int J Oral Maxillofac Implants. 2007;22(4):551–62.
41. Sotto-Maior BS, Rocha EP, de Almeida EO, Freitas-Júnior AC, Anchieta RB, Del Bel Cury AA. Influence of high insertion torque on implant placement: an anisotropic bone stress analysis. Braz Dent J. 2010;21:508–14.

42. Caglar A, Bal BT, Aydin C, Yilmaz H, Ozkan S. Evaluation of stresses occurring on three different zirconia dental implants: Three-dimensional finite element analysis. Int J Oral Maxillofac Implants. 2010;25(1):95–103.
43. Lan TH, Du JK, Pan CY, Lee HE, Chung WH. Biomechanical analysis of alveolar bone stress around implants with different thread designs and pitches in the mandibular molar area. Clin Oral Investig. 2012;16(2):363–9.
44. Coelho PG, Bonfante EA, Silva NR, Rekow ED, Thompson VP. Laboratory simulation of Y-TZP all-ceramic crown clinical failures. J Dent Res 2009;88(4):382–6.
45. Li LL, Wang ZY, Bai ZC, Mao Y, Gao B, Xin HT, et al. Three-dimensional finite element analysis of weakened roots restored with different cements in combination with titanium alloy posts. Chin Med J (Engl). 2006;119(4):305–11.
46. Cruz M, Wassall T, Toledo EM, da Silva Barra LP, Cruz S. Finite element stress analysis of dental prostheses supported by straight and angled implants. Int J Oral Maxillofac Implants. 2009;24(3):391–403.
47. Dejak B, Mlotkowski A. Three-dimensional finite element analysis of strength and adhesion of composite resin versus ceramic inlays in molars. J Prosthet Dent 2008;99(2):131–40.
48. Rees JS, Jacobsen PH. Elastic modulus of the periodontal ligament. Biomaterials. 1997;18(14):995–9.
49. Fanuscu MI, Vu HV, Poncelet B. Implant biomechanics in grafted sinus: a finite element analysis. J Oral Implantol. 2004;30(2):59–68.
50. Premnath K, Sridevi J, Kalavathy N, Nagaranjani P, Sharmila MR. Evaluation of stress distribution in bone of different densities using different implant designs: a three-dimensional finite element analysis. J Indian Prosthodont Soc. 2013;13(4):555–9.
51. Maminskas J, Puisys A, Kuoppala R, Raustia A, Juodzbalys G. The prosthetic influence and biomechanics on peri-implant strain: a systematic literature review of finite element studies. J Oral Maxillofac Res. 2016;7(3):e4.
52. Sedova A. Regulating irrational behavior in economic agents: models and strategies. Asian J Indiv Organ Behav. 2022;2(1-2022):10-4. doi:10.51847/NPJ8eR9o2M
53. Meneses-La-Riva ME, Fernández-Bedoya VH, Suyo-Vega JA, Ocupa-Cabrera HG, Grijalva-Salazar RV, Ocupa-Meneses GDD. Enhancing care quality through effective leadership in multidisciplinary healthcare teams. Ann Organ Cult Leadersh Extern Engagem J. 2023;4:54-61. doi:10.51847/9QgErkNByw
54. Sugiura T, Yamamoto K, Horita S, Murakami K, Kirita T. Micromotion analysis of different implant configuration, bone density, and crestal cortical bone thickness in immediately loaded mandibular full-arch implant restorations: a nonlinear finite element study. Clin Implant Dent Relat Res. 2018;20(1):43–9.
55. Sevimay M, Turhan F, Kiliçarslan MA, Eskitascioglu G. Three-dimensional finite element analysis of the effect of different bone quality on stress distribution in an implant-supported crown. J Prosthet Dent. 2005;93(3):227–34.
56. Sotto-Maior BS, de Andrade Lima C, Senna PM, de Villa Camargos G, Del Bel Cury AA. Biomechanical evaluation of subcrestal dental implants with different bone anchorages. Braz Oral Res. 2014;28(1):1–7.
57. Verri FR, Santiago Júnior JF, Almeida DA, Verri AC, Batista VE, Lemos CA, et al. Three-dimensional finite element analysis of anterior single implant-supported prostheses with different bone anchorages. SciWorldJ. 2015;2015(1):321528.
58. Lima de Andrade C, Carvalho MA, Bordin D, da Silva WJ, Del Bel Cury AA, Sotto-Maior BS. Biomechanical behavior of the dental implant macrodesign. Int J Oral Maxillofac Implants. 2017;32(2):264–70.
59. Agarwal A, AlRawaili AM, AlZalbani MK, AlAnazi GK, AlAnazi SK, AlEnezi SAD. A broad perspective on the role of immune-markers in gallbladder lesions: their clinico-diagnostic and prognostic significance. Asian J Curr Res Clin Cancer. 2023;3(1):34-45. doi:10.51847/NRbZvHtdPn
60. Jamal BT. Clinicopathological features and staging of oral cancer in patients seeking oral & maxillofacial surgery in Saudi Arabia. Asian J Curr Res Clin Cancer. 2023;3(2):19-24. doi:10.51847/Bjh1jzKneB
61. Theivasigamani K, Palaniappan S. Evaluation of antidiabetic drug prescribing practices in primary care clinics in rural South India. Ann Pharm Pract Pharmacother. 2023;3(1-2023):48-59. doi:10.51847/YWLWujP6kQ
62. Iftode C, Iurciuc S, Marcovici I, Macasoi I, Coricovac D, Dehelean C, et al. Therapeutic potential of aspirin repurposing in colon cancer. Pharm Sci Drug Des. 2024;4(1-2024):43-50. doi:10.51847/nyDxRaP7Au
63. Pessoa RS, Sousa RM, Pereira LM, Neves FD, Bezerra FJ, Jaecques SV, et al. Bone remodeling around implants with external hexagon and morse-taper connections: a randomized, controlled, split-mouth, clinical trial. Clin Implant Dent Relat Res. 2017;19(1):97–110.
64. Öztürk Ö, Külünk T, Külünk Ş. Influence of different implant-abutment connections on stress distribution in single tilted implants and peripheral bone: a three-dimensional finite element analysis. Biomed Mater Eng. 2018;29(4):513–26.
65. Abraha H, Philip JM. The effect of loading condition on peri-implant bone stress in regular and narrow diameter implants: a three-dimensional finite element analysis. Drug Invent Today. 2018;10(7):1243–5.
66. Santiago Junior JF, Verri FR, Almeida DA, de Souza Batista VE, Lemos CA, Pellizzer EP. Finite element analysis on influence of implant surface treatments,

connection and bone types. Mater Sci Eng C Mater Biol Appl. 2016;63:292–300.
67. Gluckman H, Du Toit J, Salama M, Nagy K, Dard M. A decade of the socket-shield technique: a step-by-step partial extraction therapy protocol. Int J Esthet Dent. 2020;15:212–25.